PHYSICAL REVIEW B VOLUME 61, NUMBER 16 15 APRIL 2000-II

Separation of interactions by noncontact force microscopy

M. Guggisberg,* M. Bammerlin, Ch. Loppacher, O. Pfeiffer, A. Abdurixit, V. Barwich, R. Bennewitz, A. Baratoff, E. Meyer, and H.-J. Güntherodt
Institute of Physics, University of Basel, Klingelbergstrasse 82, CH-4056 Basel, Switzerland
(Received 29 September 1999)

Quantitative measurements of frequency shift vs distance curves of ultrahigh-vacuum force microscopy in a noncontact mode are presented. Different contributions from electrostatic, van der Waals, and chemical interactions are determined by a systematic procedure. First, long-range electrostatic interactions are eliminated by compensating for the contact potential difference between the probing tip and the sample. Second, the long-range van der Waals contribution is determined by fitting the data for distances between 1 and 6 nm. Third, the van der Waals part is subtracted from the interaction curves. The remaining part corresponds to the short-range chemical interaction, and is found to decrease exponentially. A Morse potential is used to fit these data. The determined parameters indicate that the interaction potential between single atoms can be measured by force microscopy in a noncontact mode.

I. INTRODUCTION

Several groups have obtained images demonstrating true atomic resolution by force microscopy in a noncontact mode (nc-AFM) on different materials.[1–7] However, proper descriptions of the tip-sample interaction and contrast mechanisms are still under discussion.[8,9] The extension of nc-AFM beyond topography measurements toward a microscopy of specific surface properties depends very much on an understanding of these issues.

Various kinds of interactions, such as van der Waals (vdW), electrostatic, magnetic, and short-range chemical forces, contribute to the total force between the probing tip and sample. These interactions have different distance dependencies. One key problem in nc-AFM is to distinguish and separate these interactions. The characterization of short-range chemical forces is crucial to the understanding of true atomic resolution, and to develop procedures for single molecule manipulation.[10]

II. THEORY

In early nc-AFM papers, the observed frequency shift Δf of the oscillating cantilever was related to the gradient of the force F between the tip and sample,[11]

$$\frac{\Delta f}{f_0} = -\frac{1}{2k}\frac{\partial F}{\partial z}, \tag{2.1}$$

where f_0 is the unperturbed resonance frequency, and k is the spring constant of the force sensor. Unfortunately, this approximated equation is only valid for small tip oscillation amplitudes A, compared to the separation between probing tip and sample. For larger amplitudes the oscillation of the tip must be described by its equation of motion. If the maximum restoring force is larger than the maximum attraction $kA \gg F_{max}$, and the cantilever is driven at its shifted resonance frequency, the shift $\Delta f = f - f_0$ can be described by the following pertubation equation[8]:

$$\frac{\Delta f}{f_0} kA = \int_0^{2\pi} \frac{d\varphi}{2\pi} F(\bar{z} + A\cos\varphi)\cos\varphi. \tag{2.2}$$

The quantity on the left side of Eq. (2.2) can be measured and compared with the right side, where the force F is integrated over one oscillation cycle, and $\bar{z}$ is the time-averaged position of the tip.

To first order, the total frequency shift is the sum of the frequency shift of the different interactions $\Delta f \cong \Delta f_V + \Delta f_{vdW} + \Delta f_{chem}$, assuming that the different forces acting on the tip are additive: $F_z \cong F_V + F_{vdW} + F_{chem}$. The contribution Δf_V is caused by the long-range electrostatic interactions, while Δf_{vdW} is the contribution to the frequency shift resulting from the vdW interaction. All short-range interactions (covalent, ionic, or metallic) responsible for true atomic resolution in nc-AFM are denoted as Δf_{chem}.

In the last years, several groups have published formulas for various interactions and different tip geometries.[12–17] In this paper, we consider a conical, mesoscopic tip (half-angle α) with a spherical cap (radius R) terminated by a nanotip of height $(\bar{s} - s)$. Figure 1(a) shows a sketch of our tip model.

The electrostatic force between the mesoscopic tip and sample is written as the sum of the electrostatic forces between an infinite plane on the one hand, and the sphere and the truncated cone on the other hand. A correction term takes into account the overlap of the sphere with the cone,[18]

$$F_v = -\pi\varepsilon_0 (V_S - V_C)^2 \left\{ \frac{R}{\bar{s}} + k(\alpha)^2 \left(\ln\frac{L}{\bar{s} + R_\alpha} - 1 \right) - \frac{R[1 - k(\alpha)^2 \cos^2\alpha / \sin\alpha]}{\bar{s} + R_\alpha} \right\}, \tag{2.3}$$

where $R_\alpha = R(1 - \sin\alpha)$ is the height of the spherical cap, $k(\alpha) = 1/\ln[\cot(\alpha/2)]$, and the tip length $L \gg \bar{s}$. V_s is the voltage applied to the sample, and V_C is the surface contact potential.

An analogous procedure was used to deduce the formula for the vdW contribution. The vdW force is also the sum of

 ©2000 The American Physical Society

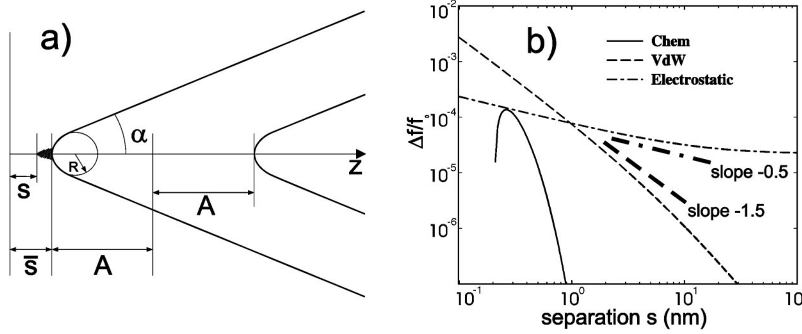

FIG. 1. (a) Tip model used in this study: conical mesoscopic tip with a spherical cap and a nanotip at the apex. R: spherical cap radius; α: half-angle of the cone. A: tip oscillation amplitude; s: separation at closest approach. (b) computed distance dependence of the normalized frequency shift for $k=30$ N/m, $A=20$ nm, $R=10$ nm, and $s=\bar{s}$. The electrostatic contribution shows an Δf vs $s^{-0.5}$ dependence; the vdW contribution exhibits Δf vs $s^{-1.5}$ in a distance range 1 nm$<s<$10 nm. The parameters in the force laws were $\alpha=100$, $V_s-V_c=1$ V, $H=4\times10^{-19}$ J, $U_0=2.27$ eV, $s_0=2.35$ Å, and $\lambda=0.79$ Å.

the vdW force between a sphere and an infinite plane, a cone and an infinite plane, and a correction term

$$F_{vdW}=-\frac{H}{6}\left[\frac{R}{\bar{s}^2}+\frac{\tan^2\alpha}{\bar{s}+R_\alpha}-\frac{R_\alpha}{\bar{s}(\bar{s}+R_\alpha)}\right], \quad (2.4)$$

where H is, to a good approximation, equal to the geometric mean of the Hamaker constants of tip and sample.[14] The same formula is obtained upon simplifying a more complicated expression derived for the same model.[19] In line with recent first-principles calculations,[21] the short-range interaction potential is represented by a Morse potential

$$U_{Chem}=U_0\left[\exp\left(-2\frac{s-s_0}{\lambda}\right)-2\exp\left(-\frac{s-s_0}{\lambda}\right)\right], \quad (2.5)$$

where s_0 is the position of the interaction potential minimum, and λ is the characteristic interaction length, expected to be less than 1 Å. The corresponding short-range interaction force is

$$F_{Chem}=\frac{2U_0}{\lambda}\left[\exp\left(-2\frac{s-s_0}{\lambda}\right)-\exp\left(-\frac{s-s_0}{\lambda}\right)\right]. \quad (2.6)$$

Using the formulas (2.3)–(2.5) for the different interaction forces, the normalized frequency shift $\Delta f/f_0$ can be calculated from Eq. (2.2). If $\bar{s}<R$, the long-range interactions are dominated by the spherical cap, i.e., the first term in the brackets on the left side of Eqs. (2.3) and (2.4). If, in addition, $A\gg\bar{s}$ one obtains simple expressions for the corresponding frequency shifts:

$$\frac{\Delta f_V}{f_0}kA=-\frac{\pi\epsilon_0 R(V_s-V_c)^2}{(2\bar{s}A)^{0.5}}, \quad (2.7)$$

$$\frac{\Delta f_{vdW}}{f_0}kA=-\frac{HR}{12\bar{s}(2\bar{s}A)^{0.5}}, \quad (2.8)$$

where $\bar{s}$ now denotes the separation between the sample and the mesoscopic part of the tip at closest approach.

A log-log plot of the normalized frequency vs distance s of the three interactions is presented in Fig. 1(b) for typical values of the parameters. In the distance range between 2 and 10 nm, the predicted power-law dependencies $\Delta f/f_0\sim\bar{s}^{-0.5}$ for the electrostatic and $\Delta f/f_0\sim\bar{s}^{-1.5}$ for the vdW contributions are verified. The influence of the short-range interactions appears only for distances shorter than 1 nm, it can be easily recognized and separated from the former contributions.

III. EXPERIMENTAL

We used a home-built multifunctional atomic force microscope operated in an ultrahigh-vacuum system.[22] Details about the instrument and the operation modes can be found in previous publications.[5,6,23] Microfabricated single-crystal Si cantilevers (phosphorus doped, 0.01–0.025 Ω cm) of rectangular shape[24] with normal spring constants k of 25–75 N/m and fundamental resonance frequencies f_0 of 150–350 kHz were used.

We adapted a frequency modulation (FM) detection scheme similar to that introduced by Albrecht *et al.*[11] The resonance frequency f was measured by a home-built FM detector.[25] The tip oscillation amplitude is maintained constant by a separate feedback circuit which controls the radio-frequency voltage applied to the piezoelement that excites the cantilever oscillation. The frequency can be precisely tuned by means of a phase shifter, in particular to track the resonance.

Clean Cu(111) surfaces were prepared according to the procedure described in Ref. 26. After the system stabilized (3 h after the preparation), two kinds of spectroscopic measurements were performed on a terrace of the Cu(111) surface. Care has been taken to avoid accidental changes of the tip apex.[23]

In order to monitor the electrostatic interaction, frequency vs bias voltage curves were recorded at different separation distances: First, a few images in the constant average tunneling current mode were recorded on the Cu(111) surface to check whether the tip is stable and can provide atomic resolution. Then the scanning process and the distance controller were stopped and a frequency vs bias curve was measured. Afterwards, the tip was retracted 1.9 nm and the same measurement was repeated several times. This procedure yields the frequency vs bias voltage at a fixed (x,y)

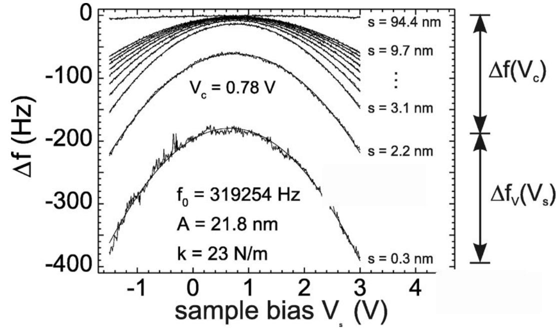

FIG. 2. Voltage dependence of the frequency shift Δf at different distances. The lowest curve was measured in a distance where tunneling current could be collected. The curves taken at $s<1.5$ nm exhibit relatively larger noise due to short-range interaction. At other distances only vdW and electrostatic interaction affect Δf.

position on the surface for different tip-sample distances s. From the maxima of these curves, the contact potential difference could be determined to be $V_c=-0.78$ V. It was found to be constant for the observed range of separations.

(2) In order to determine the vdW contribution to the frequency shift, the bias voltage was adjusted to compensate for the surface contact potential, i.e., $V_s=-V_c=0.78$ V. Frequency vs distance curves were then recorded in the following way: The tip was set near to the surface, and kept at a fixed tip-sample distance to make sure that the frequency shift was stabilized. Then the tip was retracted 5 nm from the surface, and the distance controller switched off. The tip was slowly moved toward the surface at a velocity of 2 nm/sec. The frequency shift Δf, and in addition the time-averaged tunneling current $\bar{I}_t$ between the n-doped Si cantilever and the Cu(111) sample, were recorded. At a tip sample separation where the mean tunneling current exceeds a certain value ($\bar{I}_t=7pA$), the approach was stopped and the tip was retracted. In the light of previous scanning tunneling microscopy investigations,[27] a separation $s=3$ Å was assigned to this closest approach.

IV. RESULTS AND DISCUSSION

A. Electrostatic

The electrostatic contribution is indeed proportional to the square of the applied potential difference $\Delta f_V \propto (V_s-V_c)^2$ (see Fig. 2). All measurements taken at different distances exhibit this behavior. The first Δf vs V_s curve was measured after the tip was moved toward to the surface (at $\bar{I}_t=7$ pA). This curve (closest to the surface) shows the strongest bias voltage dependence. At small separation ($\bar{s}<1.5$ nm) additional, short-range forces act on the tip and cause increased noise.

By subtracting the minimal frequency shift $\Delta f(V_c)$ from $\Delta f(s,V_s=3\text{ V})$, the contribution of the electrostatic interaction to the frequency shift can be extracted at different separation distances. The calculated Δf_V curve [Fig. 2(b)] presented in Sec. II predicts a power-law dependence $\propto s^{-0.5}$ in a separation regime between 1 and 10 nm. Fitting the measured data to a power law $C(s+\Delta s)^m$, an offset of $\Delta s=6$ nm and a slope of $m=-1.55$ were found. The distance offset of $\Delta s=6$ nm can be explained by the mesoscopic geometry of the tip, which results in an effective separation that differs from that for short-range interactions. The unexpected slope $m=-1.55$ may be explained with a frozen charge model. In the limit $A \gg \bar{s}$, the normalized frequency shift would exhibit a slope $m=-1.5$ for a pointlike charge approaching a surface with a force law $F \sim C/z^2$. As a tentative conclusion, we suggest that charges on the semiconducting tip are frozen over an oscillation period, whereas the $(V_s-V_c)^2$ dependence indicates that these charges can adjust to slow variations of V_s or s. This merits further study with coated tips of varying conductivity. From an experimental point of view, it is no problem to eliminate the electrostatic interaction by compensating for the contact potential difference with the applied voltage $V_s=-V_c$.

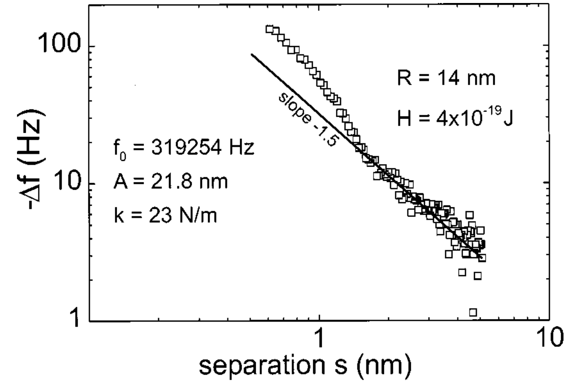

FIG. 3. Least-squares fit of the van der Waals contribution, assuming $\Delta f_{vdW} \propto \bar{s}^{-3/2}$ in the range 1–6 nm, where chemical interactions can be neglected. The cantilever was approached until the mean tunneling current exceeded a threshold 7 pA, then the tip was retracted from the surface and the frequency shift recorded. The best fit was obtained for $\bar{s}-s=0.3$ nm.

B. van der Waals interaction

Once the electrostatic part of the interaction is eliminated, the vdW and short-range chemical interactions can be determined. Beyond the range of chemical interaction ($\bar{s}>1$ nm) only vdW forces are acting on the tip. Figure 3 displays an Δf vs distance curve with compensated contact potential. In the limited range of $\bar{s}<R$ this curve can be fitted by a spherical tip model. According to Eq. (2.8) the mesoscopic radius is estimated to be about 14 nm, assuming a Hamaker constant $H=4\times10^{-19}$ J. The fit shows a good agreement with the prediction $\Delta f \propto \bar{s}^{-1.5}$ in the range $1<\bar{s}<5$ nm. In the range $\bar{s}<1$ nm the short-range interaction causes a significant systematic deviation.

C. Chemical interaction

In the last step, the short-range chemical interaction is determined by subtracting the extrapolated vdW contribution from the total frequency shift: $\Delta f_{chem}=\Delta f_{V_c}-\Delta f_{vdW}$ (Fig. 4). The resulting Δf_{chem} vs distance curve shows an abrupt but continous decrease of the frequency below a separation $s=1.2$ nm. In this range, vdW and short-range contributions grow by about the same amount. This has important consequences for the imaging process. Lateral variations of the long-range vdW contribution can affect the distance controller. For example, this can lead to incorrect apparent step heights in nc-AFM measurements.

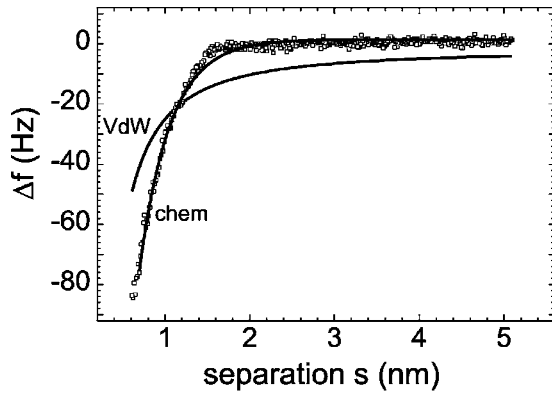

FIG. 4. Frequency shift vs distance curve after substraction of extrapolated vdW contribution. The exponential fit of the remaining frequency shift $\Delta f_{chem} = \Delta f - \Delta f_{vdW}$ for $s < 1$ nm yields a characteristic length $\lambda = 0.35$ nm and an interaction potential $U_0 = 2.35$ eV (see the text).

Since our data rarely extend below the minimum of Δf_{chem}, only the second, attractive term in of Eq. (2.6) is taken into account in the fit to the expression, which follows in the limit $A \gg s$,[8]

$$\Delta f_{chem} = -\frac{f_0}{kA}\frac{U_0}{\sqrt{\pi A \lambda}}\sqrt{2}\exp\left(-\frac{s-s_0}{\lambda}\right). \qquad (4.1)$$

The characteristic length λ is found to be 3.4 Å. The interaction strength U_0 is estimated to be 2.35 eV, assuming $s_0 = 0$. Since U_0 can be determined only up to a factor of $\exp(s_0/\lambda)$, an error of 2.5 Å in the determination of s_0 corresponds to an uncertainty of a factor of 2 in U_0. The value for U_0 is close to our expectations for the short-range interaction between a single-atom probing tip and the Cu(111) surface, and indicates that single-atom force spectroscopy is within the reach of nc-AFM. Surprisingly the characteristic length λ is significantly longer than predicted for covalent[21] or metallic adhesive interactions.[20] Similar observations of unexpectedly large decay lengths have been made on Si(111)7×7,[28,23] and on Au(111).[29] However, independent of physical interpretations we can determine the forces at closest separation $s = 0.6$ nm for the data shown in Fig. 4 to be $F_{vdW} = 1.08$ nN and $F_{chem} = 0.38$ nN.

V. CONCLUSIONS

We have demonstrated a systematic procedure for extracting parameters characterizing different types of interaction between the tip and sample. In a first step, the long-range electrostatic interaction is eliminated by compensating for the contact potential difference between the tip and sample. From the remaining long-range vdW contribution the tip radius can be estimated and used as a check on the tip shape. In the last step, the short-range interaction is determined by subtraction, and provides a measure of the range and strength of the bonding between the closest tip and sample atoms. It can therefore be used for chemical recognition on heterogeneous surfaces, as demonstrated elsewhere.[30]

ACKNOWLEDGMENTS

This work was supported by the Swiss Priority Program MINAST, Kommission für Technologie und Innovation, and by the Swiss National Foundation for Scientific Research.

*Electronic address: martin.guggisberg@unibas.ch

[1] F.J. Giessibl, Science **267**, 68 (1995).
[2] S. Kitamura and H. Iwatsuki, Jpn. J. Appl. Phys. **34**, L145 (1995).
[3] Y. Sugawara, M. Ohta, H. Ueyama, and S. Morita, Science **270**, 1646 (1995).
[4] P. Güthner, J. Vac. Sci. Technol. B **14**, 2428 (1996).
[5] R. Lüthi, E. Meyer, M. Bammerlin, T. Lehmann, L. Howald, A. Baratoff, Ch. Gerber, and H.-J. Güntherodt, Z. Phys. B: Condens. Matter **100**, 165 (1996).
[6] M. Bammerlin, R. Lüthi, E. Meyer, A. Baratoff, J. Lü, M. Guggisberg, Ch. Gerber, L. Howald, and H.-J. Güntherodt, Probe Microsc. **1**, 3 (1997).
[7] C. Loppacher, M. Bammerlin, M. Guggisberg, F. Battiston, R. Bennewitz, S. Rast, A. Baratoff, E. Meyer, and H.-J. Güntherodt, Appl. Surf. Sci. **140**, 287 (1999).
[8] F.J. Giessibl, Phys. Rev. B **56**, 16 010 (1997).
[9] A. I. Livshits, A. L. Shluger, A. L. Rohl, and A. S. Foster, Phys. Rev. B **59**, 2436 (1999).
[10] J. P. Aimé, R. Boisgard, L. Nony, and G. Couturier, Phys. Rev. Lett. **82**, 3388 (1999).
[11] T. R. Albrecht, P. Grütter, D. Horne, and D. Rugar, J. Appl. Phys. **69**, 668 (1991).
[12] S. Ciraci, A. Baratoff, and I. P. Batra, Phys. Rev. B **42**, 7618 (1990).
[13] C. Girard, Phys. Rev. B **43**, 8822 (1990).
[14] J. N. Israelachvili, *Intermolecular and Surface Forces* (Academic, London 1991).
[15] S. Ciraci, Ultramicroscopy **42-44**, 16 (1992).
[16] For an overview of force microscopy, see *Forces in Scanning Probe Methods*, Vol. 286 of *NATO Advanced Study Institute, Series E: Applied Sciences*, edited by H.-J. Güntherodt, D. Anselmetti, and E. Meyer (Kluwer, Dordrecht, 1995).
[17] U. Landmann and W. D. Luedtke, in *Scanning Tunneling Microscopy III*, edited by R. Wiesendanger and H.-J. Güntherodt (Springer, Berlin, Heidelberg 1996)
[18] S. Hudlet, M. Saint-Jean, C. Guthmann, and J. Berger, Eur. Phys. J. B. **25**, 5 (1998).
[19] C. Argento and R. H. French, J. Appl. Phys. **80**, 6081 (1996).
[20] A. Banerjea, J. R. Smith, and J. Ferrante, J. Phys.: Condens. Matter **2**, 8841 (1990).
[21] R. Perez, M. C. Payne, I. Štich, and K. Terakura, Phys. Rev. Lett. **78**, 678 (1997).
[22] L. Howald, E. Meyer, R. Lüthi, H. Haefke, R. Overney, H. Rudin, and H.-J. Güntherodt, Appl. Phys. Lett. **63**, 117 (1993).
[23] M. Guggisberg, M. Bammerlin, R. Lüthi, Ch. Loppacher, F. M. Battiston, J. Lü, A. Baratoff, E. Meyer, and H.-J. Güntherodt, Appl. Phys. A: Solids Surf. **66**, 245 (1998).
[24] O. Ohlsson, NANOSENSORS GmbH, Aidlingen, Germany.
[25] Ch. Loppacher, M. Bammerlin, F. Battiston, M. Guggisberg, D. Müller, H. R. Hidber, R. Lüthi, E. Meyer, and H.-J. Güntherodt, Appl. Phys. A: Solids Surf. **66**, 215 (1999).
[26] R. Bennewitz, V. Barwich, M. Bammerlin, Ch. Loppacher, M. Guggisberg, A. Baratoff, E. Meyer, and H.-J. Güntherodt, Surf. Sci. **438**, 289 (1999).

[27] J. A. Stroscio, R. M. Feenstra, and A. P. Fein, Phys. Rev. Lett. **57**, 2579 (1986).
[28] S. P. Jarvis, H. Yamada, S.-I. Yamamoto, H. Tokumoto, and J. B. Pethica, Nature (London) **384**, 247 (1996).
[29] G. Cross, A. Schirmeisen, A. Stalder, P. Grütter, M. Tschedy, and U. Dürig, Phys. Rev. Lett. **80**, 4685 (1998).
[30] R. Bennewitz, M. Bammerlin, M. Guggisberg, Ch. Loppacher, A. Baratoff, E. Meyer, and H.-J. Güntherodt, Surf. Interface Anal. **27**, 462 (1999).